

# Particle Size Distributions and Extinction Determined By a Unique Bistatic Lidar Technique

T. D. Stevens and C. R. Philbrick  
(tds102@psu.edu, crp3@psu.edu)

The Pennsylvania State University  
PSU/ARL Lidar Laboratory  
University Park, PA 16802  
(814) 863-0851

## INTRODUCTION

A study has been conducted to investigate the application of a unique bistatic lidar receiver to remotely determine properties of the lower tropospheric aerosols, particularly optical extinction, mean radius and size distribution width. The motivation for this study is to advance our understanding of aerosols near the ground with a possible long term goal of calculating extinction at any wavelength. Single ended remote sensing instruments, whether using lasers, radars, or microwaves, have difficulties determining absolute extinction along a propagation path. This is due to the large variations in the ratio of the forward scattering to the backward scattering between different particles (scattering phase function). The bistatic linear array receiver was developed to provide necessary information on the scattering phase function of the aerosols.

The bistatic remote receiver utilizes a linear photodiode array to image the radiation scattered from any high power CW or pulsed laser system. By observing the angular scattering variation along a horizontal path, additional information contained in the scattering angle phase function can be obtained. A technique has been developed to estimate particle size and distribution widths (of spherical scatters) by comparing two transmitted E-field components, one parallel and one perpendicular to the scattering plane. Polarizers are used on the receiver to measure the cross polarization to determine the amount of multiple scattering and nonsphericity of the particles in the scattering volume.

The first studies of this measurement technique have been conducted in a marine/coastal environment during the CASE I (Coastal Aerosol Scattering Experiment) program at the NASA flight center on Wallops Island, VA during September 1995. The atmospheric conditions during this measurement program correspond to cases of high relative humidity where the use of a spherical model to describe the scatterers would be reasonable. Results, which can be represented by trimodal lognormal size distributions, were obtained from both clear and hazy/misty nights. Extinction calculated from the size distributions is compared with extinction from the Raman lidar at two different wavelengths. On calm evenings with high humidity and decreasing temperature, the inversions also show increasing particle sizes consistent with radiation fog formation. The results

show remarkable agreement with a tri-modal aerosol distribution used in a spherical scattering model (Mie theory).

## INSTRUMENTATION AND EXPERIMENT

The linear photodiode bistatic lidar receiver is different from past bistatic lidars, which generally have the same goal of obtaining scattered radiation from the particles at angles other than  $180^\circ$ . Past experiments have used single or multiple polarizations, from a scanning laser beam to reconstruct a scattering phase function from tropospheric aerosols [1,2,3]. However, the measurement technique presented in this paper does not scan or attempt to reconstruct a scattering phase function of the particles. Instead, a ratio is obtained from the image of the scattering of two orthogonal polarization components with respect to angle, one in the scattering plane and one perpendicular to the scattering plane along a horizontal path, as shown in Fig.1. The use of a ratio cancels the effects of

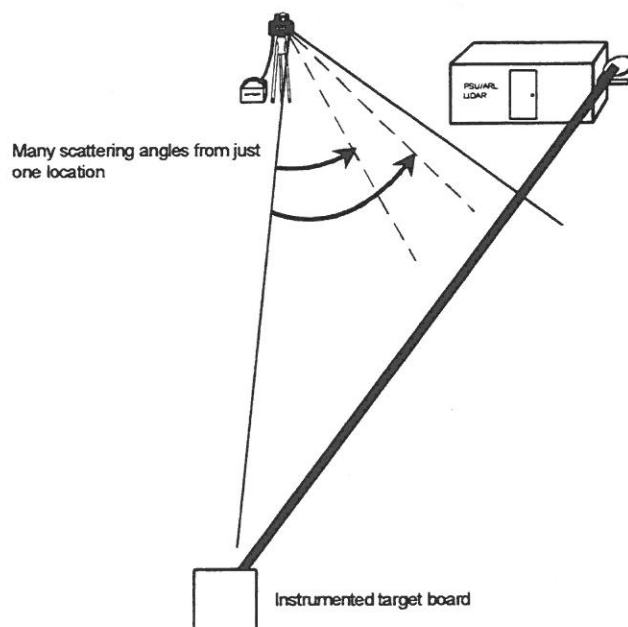


Figure 1. By operating in the horizontal mode, the bistatic lidar is able to collect radiation from many scattering angles, between  $155^\circ$  and  $180^\circ$ , from just one location.

many problems, including nonlinearities across the field of view of the receiver and extinction differences due to different path lengths for each scattering angle. Fig.1 demonstrates the ability of the bistatic receiver to simultaneously image the backscattered radiation from an angle range of  $155^\circ$  to  $180^\circ$ . The assumption of a uniform horizontal path is verified with horizontal extinction profiles from the monostatic Raman lidar during each data set [4,5]. Although this polarization ratio contains the information needed to characterize the scatterers, a model is needed to relate this ratio to the desired parameters, such as extinction, and particle size distribution.

One of the goals of this research was to determine how well Mie theory, with a lognormal distribution of scatterers would describe actual aerosol data, in a humid coastal/marine environment. A program was written using several subroutines including BHMIE from [6], that modeled the ratio of the two polarization components from the bistatic lidar with a trimodal lognormal distribution of spherical scatterers. It was discovered that in order to accurately model the return from a clear night, the molecular scattering component had to be added to the aerosol distribution. Fig.2 shows a sample lognormal particle size distribution including the addition of  $2.54 \times 10^{25}$  molecules per  $m^3$ , at a radius of 0.198 nm.

The first tests of this measurement technique were conducted in September 1995, during the CASE I (Coastal Aerosol Scattering Experiment) on Wallops Island Virginia. This location was chosen for its humid and misty, coastal/marine environment, and for an unobstructed 3.28 km horizontal path over a salt marsh. The Penn State LAMP (Laser Atmospheric Measurement Program) monostatic lidar, [7], was operated on both a horizontal path and a vertical path. When operating on a horizontal path the LAMP lidar collected rotational Raman temperature profiles, vibrational Raman water vapor profiles, vibrational Raman nitrogen profiles, and aerosol/molecular scattering profiles at the fundamental laser wavelength of 532 nm.

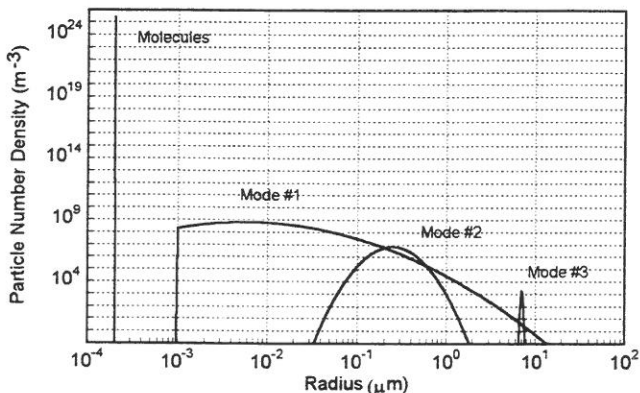


Figure 2. A plot of a trimodal lognormal particle size distribution using the bistatic lidar model. The addition of  $2.54 \times 10^{25}$  molecules per  $m^3$  is shown at the "equivalent Mie radius" of 0.198 nm.

The bistatic receiver and the laser were separated by 15.24 m which imaged the scattering path between 35 m and 175 m, and corresponded to scattering angles between  $155^\circ$  and  $175^\circ$ . The distance from 175 m to 3.28 km corresponds to an angle range of  $175^\circ$  to  $180^\circ$ , so one must use care when analyzing data from this range, because the horizontal path is more likely to be uniform over 140 m than over 3 km.

## DATA ANALYSIS AND RESULTS

Data were collected under a range of conditions, from dry and clear to damp and misty, during the Wallops CASE I program. However, the most interesting data were collected on September 14, 1995, a calm, damp and hazy evening. Fig.3b shows a plot from 11:00 pm to 3:00 am of the temperature and relative humidity versus time. The wind speed is indicated in miles per hour next to each temperature data point. Here we can see the relative humidity remains constant at about 90% until about 1:30 am, while the temperature slowly dropped from  $23^\circ\text{C}$  to  $22^\circ\text{C}$ . After 1:30 am the wind speed increased to 5 mph and brought with it a warmer and drier air mass. The temperature decrease of  $1^\circ\text{C}$  does not seem like a large change, but from

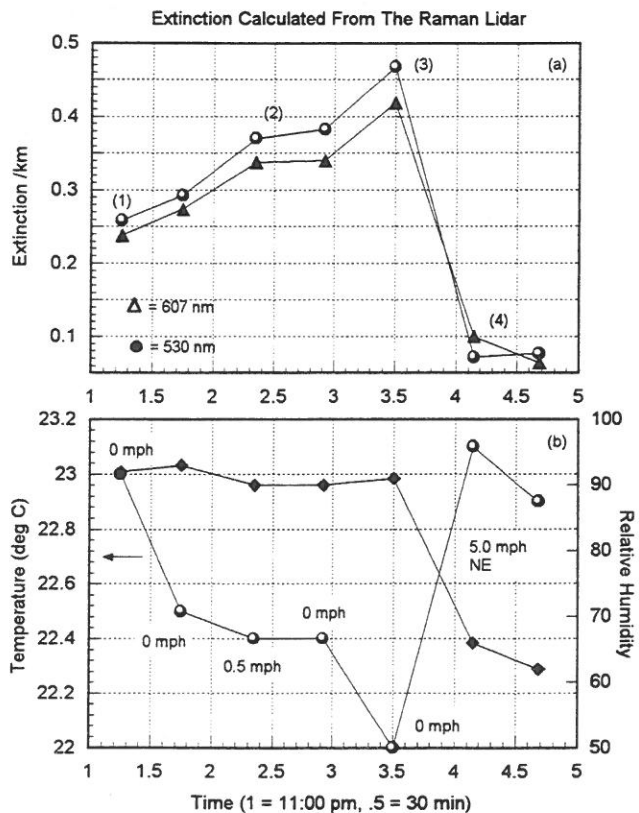


Figure 3. (b) A plot of the temperature and relative humidity versus time from the lidar weather station on the night of September 14, 1995. (a) Corresponding plots of extinction coefficients from the Raman lidar at 607 and 530 nm, at the same times as the temperature and relative humidity plots (b).

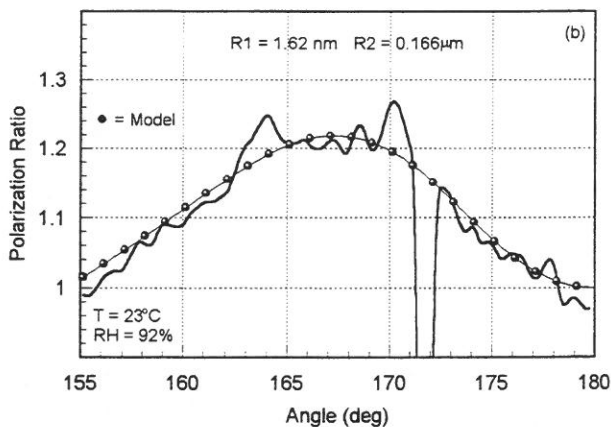
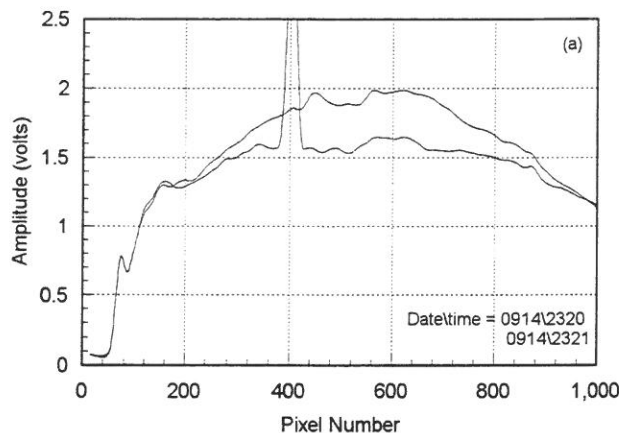


Figure 4. (a) A plot of the two electric field components measured with the bistatic lidar on September 14, 1995. (b) The ratio of the two polarization components in (a) shown with the best first order fit from the model.

Fig.3a, it is apparently large enough to cause significant changes in the average extinction coefficient calculated from the Raman 607 and 530 nm lidar channels. Prior investigations [4,5] present the analysis for determining absolute extinction from a Raman lidar return.

Fig.4a shows a plot of the unprocessed data for two polarization components measured with the bistatic lidar early in the evening at 11:20 pm, corresponding to the first data point in Fig.3. Because the two polarization components are separated in time by one minute, spikes in the data, like the one at pixel number 400, can occur when an insect flies through the laser beam. Fig.4b shows the ratio of the two components in Fig.4a with a solid dark line, accompanied by the best first order fit of the model. The first order fit with two aerosol modes is found by adjusting the six lognormal distribution parameters, with a fixed index of refraction ( $n=1.38$ ), until the sum of the differences between the model and the data is minimized. On a clear night, with only a single mode of small aerosols, the number density of the molecules can be used as the absolute reference to tie off the number density of the aerosol distribution. On this night however, the second mode of the

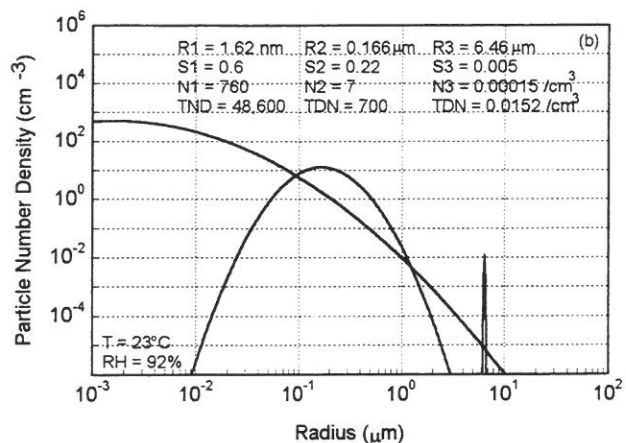
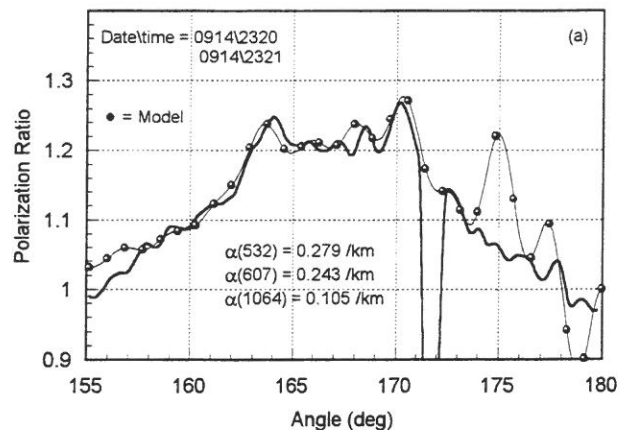


Figure 5. (a) A good trimodal fit of the model (dotted line) to the data showing a nearly monodispersed radiation fog forming. (b) The lognormal distributions, with an index of refraction of 1.38, used to fit the model to the data in (a).

aerosol distribution, not the molecules, is dominating the scattering. The extinction calculated from the Raman lidar, shown as the first point in Fig.3a is used to normalize the number densities of the first two modes of the distribution. The presence of the high frequency ripples versus angle in Fig.4b is an indication that a third larger particle mode is contributing to the scattering. This last mode was extremely difficult to find because the standard third modes described in the literature did not improve the fit. Finally, very narrow distributions were tried, and an excellent match was found with a particle radius of  $6.46 \mu\text{m}$ , and a distribution width of only  $\log\sigma = .005$ , as shown in Fig.5. Nearly monodispersed particle distributions like these are often called radiation fog, and generally form from the condensation of water vapor molecules onto the surface of particles as the temperature drops on calm, humid nights. The trimodal lognormal distribution that best matches this data set is shown in Fig.5, with TND referring to the total particle number density for that mode.

Because this evening was calm with zero wind speed, it can be assumed that the particle number density will not significantly change throughout the course of the night. If the particle

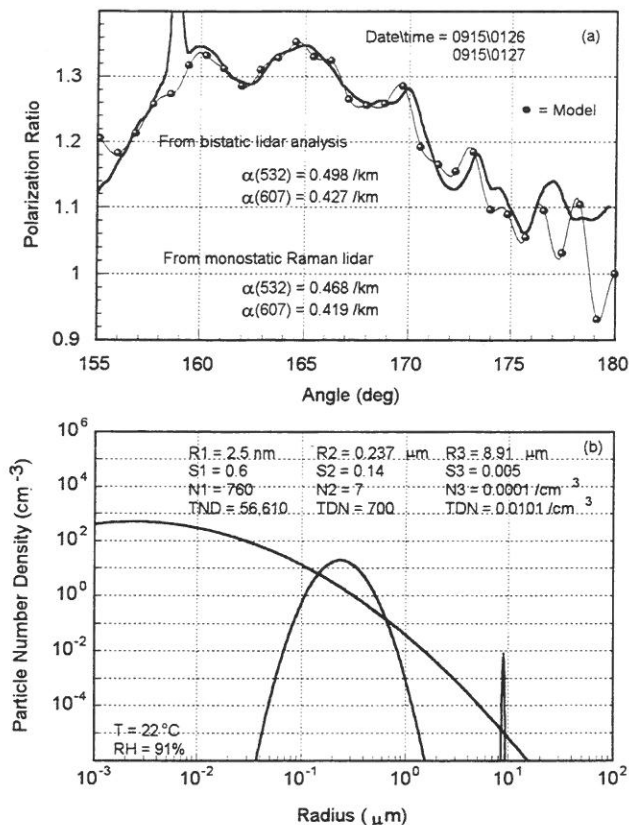


Figure 6. (a) A most convincing example of this bistatic lidar measurement technique, showing the best fit of the spherical model, using the distribution from (b), with the data. The radiation fog mean radius has grown from 6.46  $\mu\text{m}$  to 8.91  $\mu\text{m}$  in only 2.5 hours.

number density does not change, then only the radius and distribution width of the three aerosol modes should be altered to fit the model to each consecutive data set. Five bistatic lidar data sets were inverted for particle size distributions which show the increasing radius of each particle as the temperature dropped and the extinction increased. The last data set to be inverted for a trimodal lognormal particle size distribution corresponds to point 3 in Fig. 3a and is shown in Fig. 6.

Probably the most convincing example of this measurement technique is shown in Fig. 6a, with the best fit of the model, and the corresponding trimodal distribution in Fig. 6b. The temperature decreased while the extinction increased one last time before the wind brought a new air mass and different scatterers in the area. The second mode of the distribution is seen to narrow its distribution width as it grows from a radius of 0.166  $\mu\text{m}$  to 0.237  $\mu\text{m}$ . At the same time the third mode increases from a radius of 6.46  $\mu\text{m}$  to 8.91  $\mu\text{m}$ . This data set is most striking because the model follows almost every contour in the data between 155° and 180° as seen in Fig. 6a. Not only does the model fit the data almost perfectly after increasing only the mode radii, but the calculated extinction coefficients are also

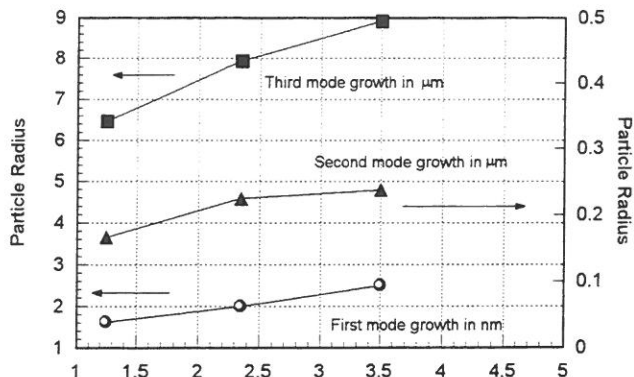


Figure 7. A summary of the growth of the particles through the night, as determined from inverting the data from the bistatic lidar.

the same as those measured by the Raman lidar, see extinction data in Fig. 6a. Fig. 7 summarizes the growth of the three modes throughout the evening before a new air mass entered the measurement area and the conditions changed from cold and humid, to warm and dry.

#### ACKNOWLEDGMENTS

Special appreciation for the support of this work goes to Dr. Juergen Richter of NCCOSC Nrad, and to Dr. Geary Schwemmer of NASA GSFC. The efforts of Dr. Balsiger, Savy Mathur, Mike O'Brien, Dr. Ruf, Dr. Kunz, Dr. Aydin, Dr. Lyask, and Dr. Bohren have contributed much to the success of this project.

#### REFERENCES

- [1] J.A.Reagan, and B.M.Herman, "Bistatic lidar investigations of atmospheric aerosols," Proc. Conf. Radar Meteorol., 14th, p.275, 1970.
- [2] P.C.S.Devara, and P.Ernest Raj, "A bistatic lidar for aerosol studies," IETE Tech. Rev. Vol. 4, p.412, 1987.
- [3] K.Parameswaran, K.D.Rose, and B.V.Krishna Murthy, "Aerosol characteristics from bistatic lidar observations," J. Geophys. Res. Vol. 89, No. D22, p.2541, 1984.
- [4] T.D.Stevens, and C.R.Philbrick, "Atmospheric extinction from Raman lidar and a bistatic remote receiver," Proc. Conf. IEEE topical Symp. CO-MEAS, p.170, 1995.
- [5] C.R.Philbrick, "Raman lidar measurements of atmospheric properties," Proc. of Atm. Prop. and Remote Sensing III, SPIE 2222, p.922, 1994
- [6] C.F.Bohren, and D.R.Huffman, Absorption and Scattering of Light by Small Particles, Wiley-Interscience, New York, 1983.
- [7] C.R.Philbrick, D.B.Lysak, T.D.Stevens, P.A.T.Haris and Y.-C.Rau. "Atmospheric measurements using the LAMP lidar during the LADIMAS campaign," Proc. of the 11th ESA Symp. ESA-SP-355, p.223, 1994.